ALEPH 92-130
PHYSIC 92-119
H. Meinhard et al.
30.7.1992

Reducing the Statistical Error on the Z Width Through Use of a Relative Luminosity Measurement

H. Meinhard
CERN - Geneva

T. Fearnley, D. Hansen, and P. Hansen
Niels Bohr Institute - Copenhagen

E. Barberio
Universität Siegen - Seigen

W. Chen and J. Harton
University of Wisconsin-Madison

July 30, 1992

Abstract

We report on a method to measure the relative luminosity in ALEPH. The acceptance for Bhabha events of the relative method is about 1.4 times that for the standard selection method. The increase in acceptance allows for reduction in the statistical errors on cross sections. The statistical error on the Z width is consequently reduced by about 1 MeV for the 1990 and 1991 data.

1 Introduction

The measured cross section for Z decay into $q\bar{q}$ pairs may be written as

$$\sigma_{z\to q\bar{q}} = \frac{N_{had}/\epsilon_{had}}{N_{bha}/\sigma^{mc}_{bha}}$$

where N_{had} is the number of accepted hadronic events, N_{bha} is the number of accepted Bhabha events, σ^{mc}_{bha} is the Bhabha cross section from Monte Carlo, and ϵ_{had} is the efficiency for hadron selection. The statistical error on $\sigma_{z\to q\bar{q}}$ is

$$\Delta\sigma_{z\to q\bar{q}} = \sigma_{z\to q\bar{q}}\sqrt{1/N_{had} + 1/N_{bha}}$$

Here we have ignored the very small contribution to the error from the background in the Bhabha sample.

In this note we present a new method for Bhabha selection for which N_{bha} is increased with respect to the standard method for Bhabha selection. In this way $\Delta\sigma_{z\to q\bar{q}}$ is reduced. Consequently the statistical errors on the Z mass and width are also reduced.

The new method is used to reduce the statistical uncertainty on cross section points relative to each other. The standard method is used to set the overall absolute luminosity (i.e. summed over center of mass energies), and hence the overall scale for the cross sections.

2 The apparatus

In the relative luminosity measurement, LCAL is used as usual. A description of LCAL can be found in ref. [1]. As in previous work SATR is used for systematic checks.

The active area of an LCAL module, including the fiducial (hatched) and non-fiducial (dash outline) boundaries, is shown in figure 1.

3 Event selection

In our selection of Bhabha events, we remain close to the well-tested standard method (M8) [1]. A comparison between our new selection method and that of M8 is shown in table 1. The only difference between the methods is that for the relative luminosity we remove the fiducial cut (side 1) in order to accept more events. The non-fiducial cut (side 2) is still applied. As in the standard method, side 1 and side 2 alternate for every trigger.

Figures 2-5 show comparisons of Monte Carlo (BHLUMI generator) to 1991 data for the relative luminosity method. In each plot all cuts are applied except the cut on the quantity plotted. The Monte Carlo is shown as a solid histogram, and the data is shown as points (background, order 10^{-4}, is not subtracted).

4 Influence of beam parameters

In the standard method there is a well defined difference in the size of the fiducial and the non-fiducial area (see figure 1). For the relative luminosity, as explained above, there is no

position cut on clusters on side 1. On side 2 the non-fiducial requirement is applied. Since clusters near the edge of the detector lose energy, it is not a priori clear if a correlation between energy and position might effectively reduce the size of the acceptance on side 1 to the same size as that for side 2. If this were the case then the uncertainty in relative luminosity due to beam positions and angles would be larger than the corresponding uncertainty in the absolute luminosity. Figure 6 shows the average energy of clusters near the horizontal plane as a function of horizontal position (as measured by SATR). There is a clear difference in size for sides 1 and 2, of the order of 0.5 cm.

This effect has been studied in a toy Monte Carlo in which the energy-position correlation of figure 6 has been taken into account. The toy Monte Carlo also used the measured beam positions, listed in table 2. The average measured energy stays above 60% down to 40mr. At the loose cut (46mr), the average energy is 86%. So the loose cut really removes some acceptance (20%) - independently of the energy cut.

For the toy Monte Carlo we used two selections: in the first we only cut on the energy, while in the second we cut on the energy, and applied an alternating non-fiducial cut. The second method rejects 20% of the events accepted by the first toy method. Table 3 shows the estimates of the systematic errors for the two toy Monte Carlo methods. With the asymmetric position cut, the largest error is 0.1 per mille. Also, the horizontal beam direction is known to be controlled to 0.25mrad within a fill. Such a tilt changes the luminosity by 0.1 per mille. Similarly, from the vertical beam direction, we found a change of 0.2 per mille. These are maximal deviations from the design orbit, so it is not unreasonable to assume that the average orbits over different sets of fills are equal within those limits. All together the systematic error from point to point is at most 0.3 per mille.

5 Beam-related background and $\Delta\phi$ efficiency

The background from off momentum beam particles for standard method selection is very low. We want to make sure whether this is still true for the new method. Studies of 1990 and 1991 data indicate that the fraction of beam-related background is always less than 0.3 per mille at each energy point for both years. The difference in this fraction between two methods is always less than 0.05 per mille for 1991 data and 0.09 per mille for 1990. The ratios of beam-related background for 1991 data are shown in figure 7 and those for 1990 data are shown in figure 8 for both methods.

The $\Delta\phi$ efficiency, which is the ratio of the number of events passing all of the cuts except the $\Delta\phi$ cut to the total number of events passing all the cuts, is another sensitive test of the new method. The efficiencies for 1991 and 1990 data are shown in figure 9 and figure 10 respectively. Energy-independence is confirmed to the level of 1 per mille for both methods in both years. In figure 7 - 10, The ratios for new method are shown as shaded circles and those for standard method are shown as open circles.

6 Electroweak corrections

The luminosity at a given energy point i, measured using method m, can be written

$$\mathcal{L}_i^m = \frac{N_i^m}{\sigma_i^m} = \frac{N_i^m s_i}{\sigma_{ref}^m s_{ref} c_i^m}$$

Here, N_i^m denotes the number of accepted events for method m, and σ_i^m is the accepted cross section for this method. σ_{ref}^m is the accepted cross section for method m at some reference energy, which must be corrected for center of mass energy by s_{ref}/s_i as well as for an electroweak correction c_i^m. This electroweak correction is normalized to 1.0 at the reference energy, mass and width.

The size of the electroweak correction depends on the method; the method with the largest inner radius cut has the largest correction. The effective inner radius of method 10 is only about 5 *mm* smaller than that of method 8, giving a slightly smaller energy variation for method 10 than for method 8. Figure 11 shows the relative difference in electroweak corrections between method 10 and method 8, as a function of energy [2]. The largest difference is seen to be 0.25 per mille. An independent evaluation of the difference in electroweak correction between the standard method and the new method also shows that the largest difference is about 0.2 per mille [3].

7 How to make use of the relative luminosity

To obtain an absolute luminosity, we require that the sum of the luminosities over the energy points to be equal for the standard (M8) and the relative (M10) method:

$$\sum_i \mathcal{L}_i^8 = \sum_i \mathcal{L}_i^{10}$$

The following equation, after inserting the above expression, allows for the elimination of the yet unknown reference cross section of the relative method:

$$\frac{1}{\sigma_{ref}^{10}} = \frac{1}{\sigma_{ref}^8} \frac{\sum_k (N_k^8 s_k / c_k^8)}{\sum_k (N_k^{10} s_k / c_k^{10})}$$

The luminosities as determined by the relative method become

$$\mathcal{L}_i^{10} = \frac{1}{\sigma_{ref}^8} \frac{\sum_k (N_k^8 s_k / c_k^8)}{\sum_k (N_k^{10} s_k / c_k^{10})} \frac{N_i^{10} s_i}{s_{ref} c_i^{10}}$$

Trying to estimate the gain in the precision of the cross sections, we disregard for the moment the slight energy weighting which is included in the ratios of the sums

$$\frac{\sum_k (N_k^8 s_k / c_k^8)}{\sum_k (N_k^{10} s_k / c_k^{10})}$$

The additional electroweak corrections are neglected as well. Since about 300 000 Bhabha events were accepted by the standard method for the runs selected for electroweak physics in 1991, and about 450 000 were selected by the relative method, which comprise the 300 000 of the standard method completely, the relative error of that ratio is of the order of 1 per mille. We suggest to add this to the systematic error of the luminosity. Its contribution to the total systematic error is negligible.

Comparing the statistical error on the hadronic cross sections as determined with the standard luminosity to the statistical error obtained using the relative luminosity, the latter error is found to be smaller by 3 to 8 percent. This number takes into account the additional error contribution from the overall normalization, which appears in the relative method.

As the number of Bhabha events accepted by the relative method enters into the hadronic cross sections both directly and through the normalization factor, correlations must be handled with care. A full calculation, however, shows that their effect is negligible, and that the error due to the normalization factor may be added in quadrature, allowing us to consider this error an additional contribution to the systematic error of the luminosity.

8 Results

The cross section for the standard method (M8) is $\sigma_{m8} = 26.35 \pm 0.03\, nb$, while the cross section for the relative luminosity is $\sigma_{relative} = 38.42 \pm 0.04\, nb$. N_{bha} increases by a factor of about 1.46 at each energy point. Expected improvement in statistical errors are shown in table 4.

We test the stability of the relative luminosity in the same way as for the standard method. We vary the cuts, and get the ratio of the relative luminosity after the variation to that before the variation, which is shown in table 5. Thus the relative method is stable to the level of 0.7% even if used as an absolute luminosity measurement.

Finally we calculate the ratio of the luminosity from the new method to that of the standard method at each energy point, for 1991 data. The results are shown in figures 12 - 14 and tables 6 - 8. The final results for 1990 data are shown in figure 15 and table 9. The overall level of the relative luminosity is set at that of M8. This means we sum up the luminosity at each energy point for both the standard and the new method to get the constant α, which is the ratio of the total luminosity of M8 to that of M10. We then multiply the raw luminosity of the new method at each energy point by α to get the final, normalized luminosities for the new method. Both the raw and the normalized luminosities for the new method are included in table 6 - 9. Only normalized luminosities are shown in figures 12 - 15.

9 Conclusions

A simple and stable relative luminosity measurement for ALEPH has been presented. The absolute scale is determined by normalizing to the standard (M8) luminosity. By using the relative luminosity, we reduce the statistical error on both the mass and the width of the Z by 1 MeV, which is equivalent to 15% more data in 1991. For 1990 data, the statistical error on the total Z width goes down from 18 Mev to 17 Mev.

10 References

1. "Measurement of the absolute luminosity with the ALEPH detector", D. Decamp et al., Z phys. C - Particles and fields 53, 375-390 (1992).

2. "Energy dependence of radiative and electro-weak corrections to the Bhabha cross section", J.D. Hansen, J.R. Hansen and B. Pietrzyk, ALEPH 92-75 PHYSICS 92-66 (27.5.1992).

3. B. Pietrzyk, private comm.

11 Figure captions

Figure 1: The definition of fiducial side cut and non-fiducial side cut.
Figure 2: Energy distribution normalized to E_{beam} for side 1.
Figure 3: Energy distribution normalized to E_{beam} for side 2.
Figure 4: Total energy distribution normalized to E_{cms}.
Figure 5: The difference in azimuth angle, $\Delta\phi$, between the two clusters (on side 1 and side 2) for the new method.
Figure 6: Average LCAL energy versus X coordinate (from SATR) for tracks near the horizontal plane, at $|z| = 280cm$. Only good SATR tracks are used. 1991 data only.
Figure 7: Fraction of beam-related background of both methods for 1991 data. Open circles show the standard method, closed circles show the relative method.
Figure 8: Fraction of beam-related background of both methods for 1990 data. Open circles show the standard method, closed circles show the relative method.
Figure 9: $\Delta\phi$ efficiency of both methods for 1991 data. Open circles show the standard method, closed circles show the relative method.
Figure 10: $\Delta\phi$ efficiency of both methods for 1990 data.Open circles show the standard method, closed circles show the relative method.
Figure 11: Relative difference between method 10 and method 8 electroweak corrections, in per mille, as a function of LEP energy.
Figure 12: Ratio of luminosities for all 1991 data.
Figure 13: Ratio of luminosities for each run whose run number is less than 12341. (These are the pre-scan runs.)
Figure 14: Ratio of luminosities for each run whose run number is greater than 12438. (These are the runs taken during the Z-scan.)
Figure 15: Ratio of luminosities for all 1990 data.

Table 1: Selection cuts

STANDARD METHOD (M8)	RELATIVE LUMINOSITY
$E_i > 0.22\sqrt{s}$ $(i = side1, 2)$	Same
$E_1 + E_2 > 0.6\sqrt{s}$	Same
$170.0 < \Delta\phi < 190.0$	Same
Non-fiducial side cut	Same
Fiducial side cut	Do not make this requirement

Table 2: The average vertex measured by track detectors in 1991

Energy	N_{had}	V_x	rms	V_y	rms	V_z	rms
88.5	3647	-0.099	0.013	0.068	0.007	0.076	0.214
89.5	7904	-0.110	0.016	0.069	0.006	0.062	0.228
90.25	13426	-0.086	0.020	0.065	0.008	-0.025	0.188
91.25	233005	-0.102	0.009	0.069	0.008	-0.009	0.100
92.0	17222	-0.106	0.011	0.067	0.008	0.062	0.110
93.0	9758	-0.102	0.011	0.069	0.006	0.042	0.113

Table 3: Error from point to point, per mille.

Energy(Gev)	cut on energy only	cut on energy and asym. position cut
88.5	0.214 $\pm$ 0.024	-0.050 $\pm$ 0.008
89.5	-0.194 $\pm$ 0.023	0.110 $\pm$ 0.020
90.25	0.767 $\pm$ 0.045	0.025 $\pm$ 0.007
92.0	0.008 $\pm$ 0.011	-0.025 $\pm$ 0.004
93.0	0.122 $\pm$ 0.018	0.000 $\pm$ 0.003

Table 4: The gain in Z mass and Z width errors for 1991 data

Method	$\Delta\Gamma_z$(Mev)	ΔM_z(Mev)
Standard (m8)	16	9
New	15	8

Table 5: Stability of relative luminosity for 1991 data

Variation of cuts	L'/ L
$150.0 < \Delta\phi < 210.0$	1.0005
$E_1, E_2 > 0.56\sqrt{s}$,$E_1 + E_2 > 0.78\sqrt{s}$	1.0019
$E_1, E_2 > 0.36\sqrt{s}$,$E_1 + E_2 > 0.5\sqrt{s}$	1.0010
Looser non-fiducial boundary	1.0064
Total	1.0068

Table 6: Final results for 1991 data ($\alpha = 0.99249$)

Energy(Gev)	N_{ms}	N_{new}	$L_{ms}(nb^{-1})$	$L_{new-raw}(nb^{-1})$	$L_{new-final}(nb^{-1})$
88.464	18809	27736	668.375	676.089	671.014
89.456	21963	32347	796.770	804.973	798.931
90.212	20418	29804	753.217	754.201	748.540
91.226	198918	292146	7545.887	7602.248	7545.187
91.952	17890	26317	693.216	699.520	694.270
92.952	17063	25161	677.310	685.119	679.977
93.701	19047	27862	768.179	770.823	765.037

Table 7: For each run whose run number is less than 12341 ($\alpha = 0.99343$)

Energy(Gev)	N_{ms}	N_{new}	$L_{ms}(nb^{-1})$	$L_{new-raw}(nb^{-1})$	$L_{new-final}(nb^{-1})$
90.240	2349	3462	86.712	87.666	87.090
91.238	121449	178203	4608.805	4638.903	4608.428

Table 8: For each run whose run number is greater than 12438($\alpha = 0.99189$)

Energy(Gev)	N_{ms}	N_{new}	$L_{ms}(nb^{-1})$	$L_{new-raw}(nb^{-1})$	$L_{new-final}(nb^{-1})$
88.464	18809	27736	668.375	676.089	670.603
89.456	21963	32347	796.770	804.973	798.441
90.208	18069	26342	666.499	666.531	661.122
91.207	77469	113943	2937.066	2963.326	2939.279
91.952	17890	26317	693.216	699.520	693.844
92.952	17063	25161	677.310	685.120	679.560
93.701	19047	27862	768.179	770.822	764.567

Table 9: Final results for 1990 data ($\alpha = 0.99505$)

Energy(Gev)	N_{ms}	N_{new}	$L_{ms}(nb^{-1})$	$L_{new-raw}(nb^{-1})$	$L_{new-final}(nb^{-1})$
88.212	13456	19783	481.911	482.581	480.191
89.209	14221	20995	520.033	522.918	520.329
90.213	11962	17526	447.133	446.204	443.994
91.214	90976	134573	3495.751	3522.029	3504.589
92.211	14031	20672	554.640	556.582	553.826
93.217	14767	21673	597.332	597.128	594.171
94.214	15544	22924	641.919	644.813	641.619

FIGURE 1

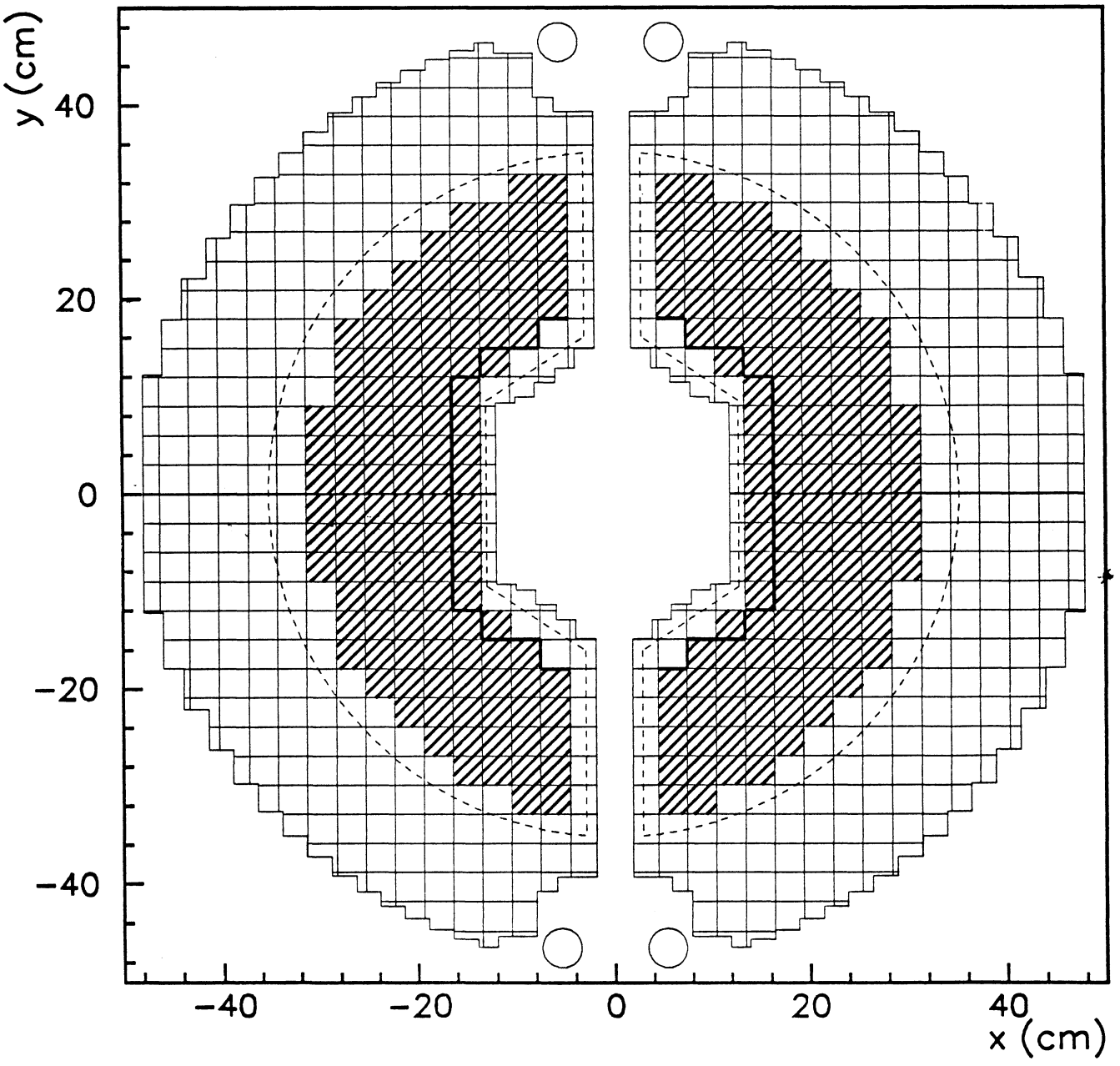

FIGURE 2

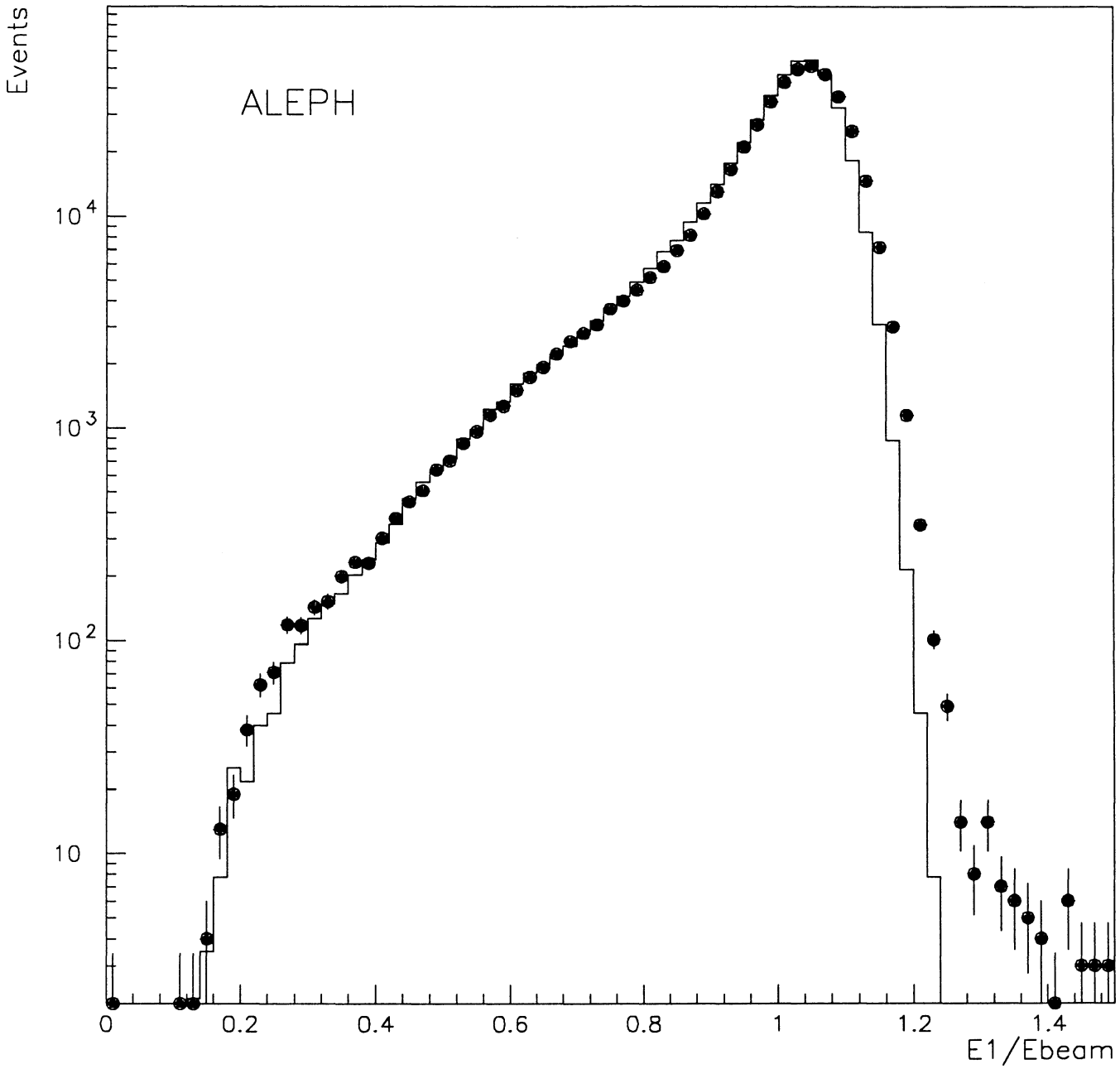

FIGURE 3

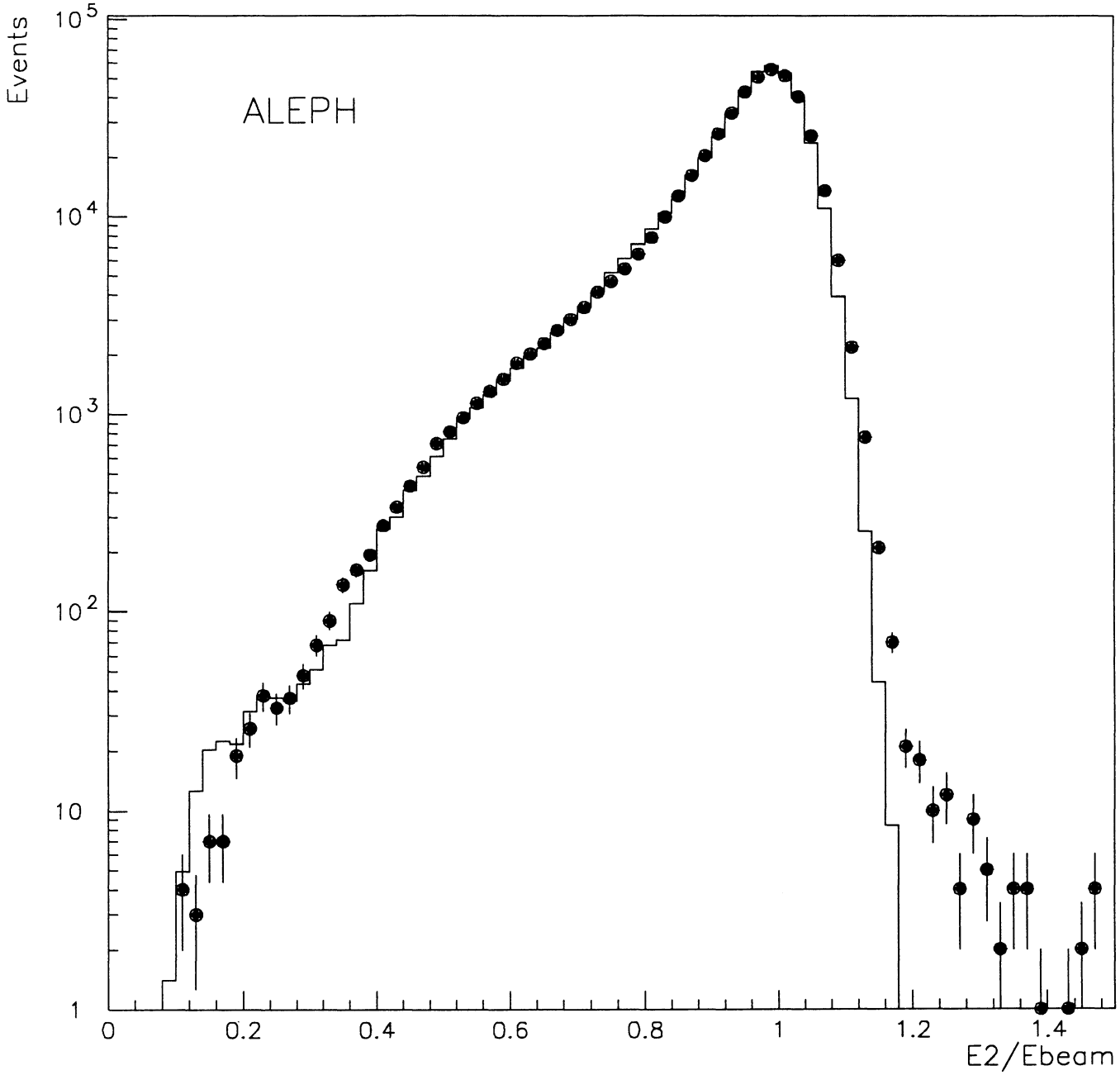

FIGURE 4

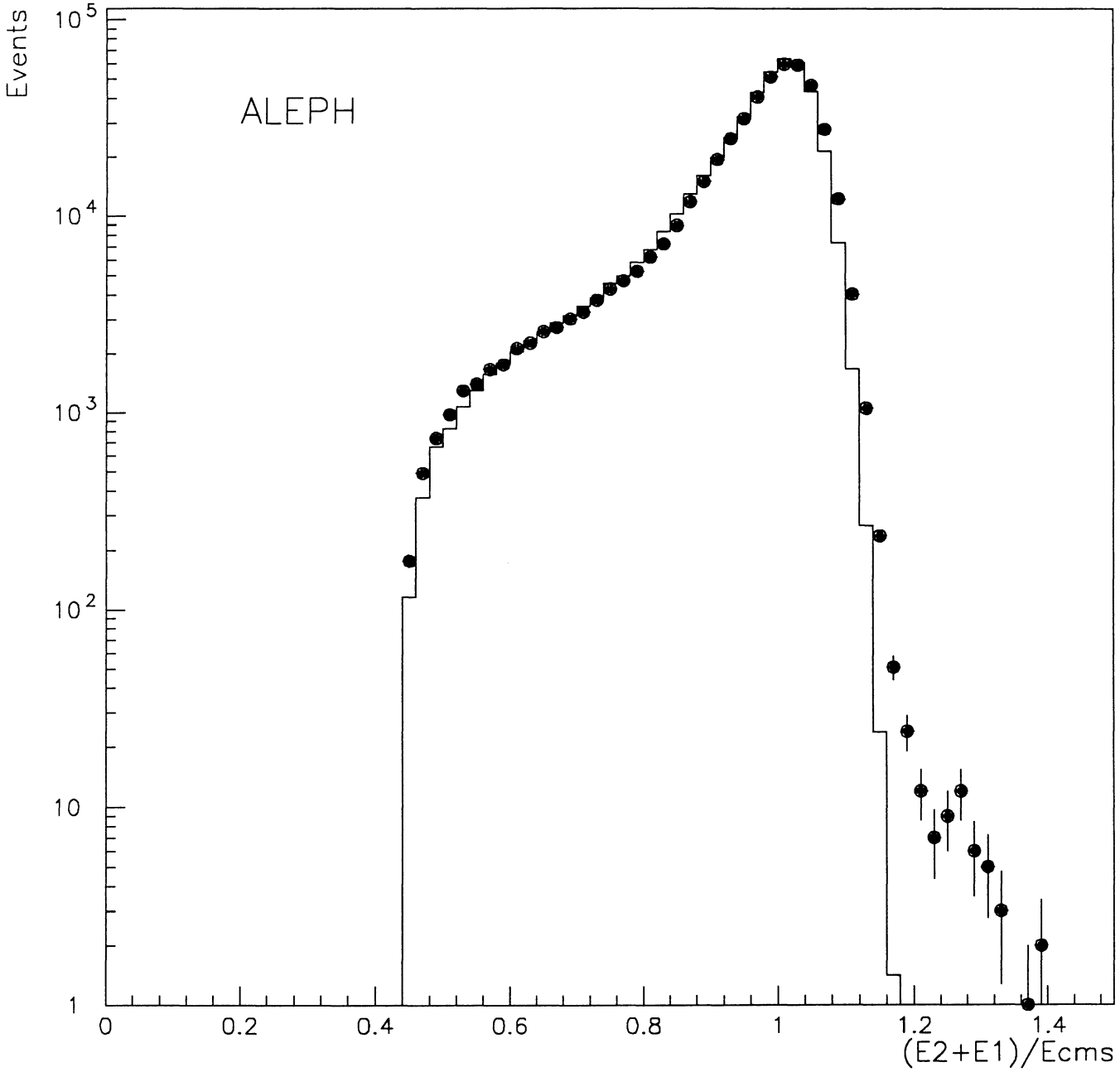

FIGURE 5

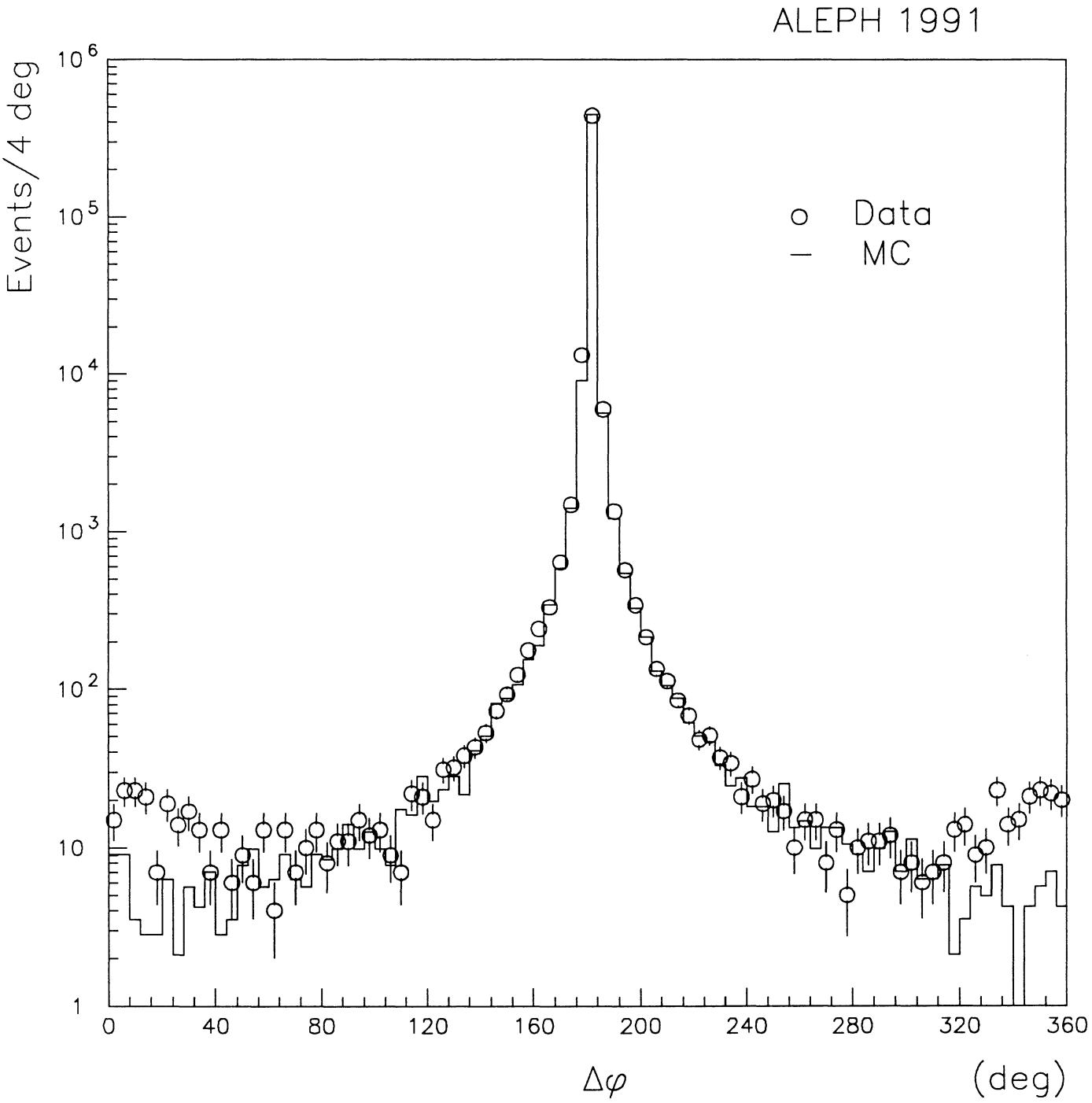
ALEPH 1991
Events/4 deg
10^6
10^5
10^4
10^3
10^2
10
1
o Data
— MC
0
40
80
120
160
200
240
280
320
360
$\Delta\varphi$
(deg)

FIGURE 6

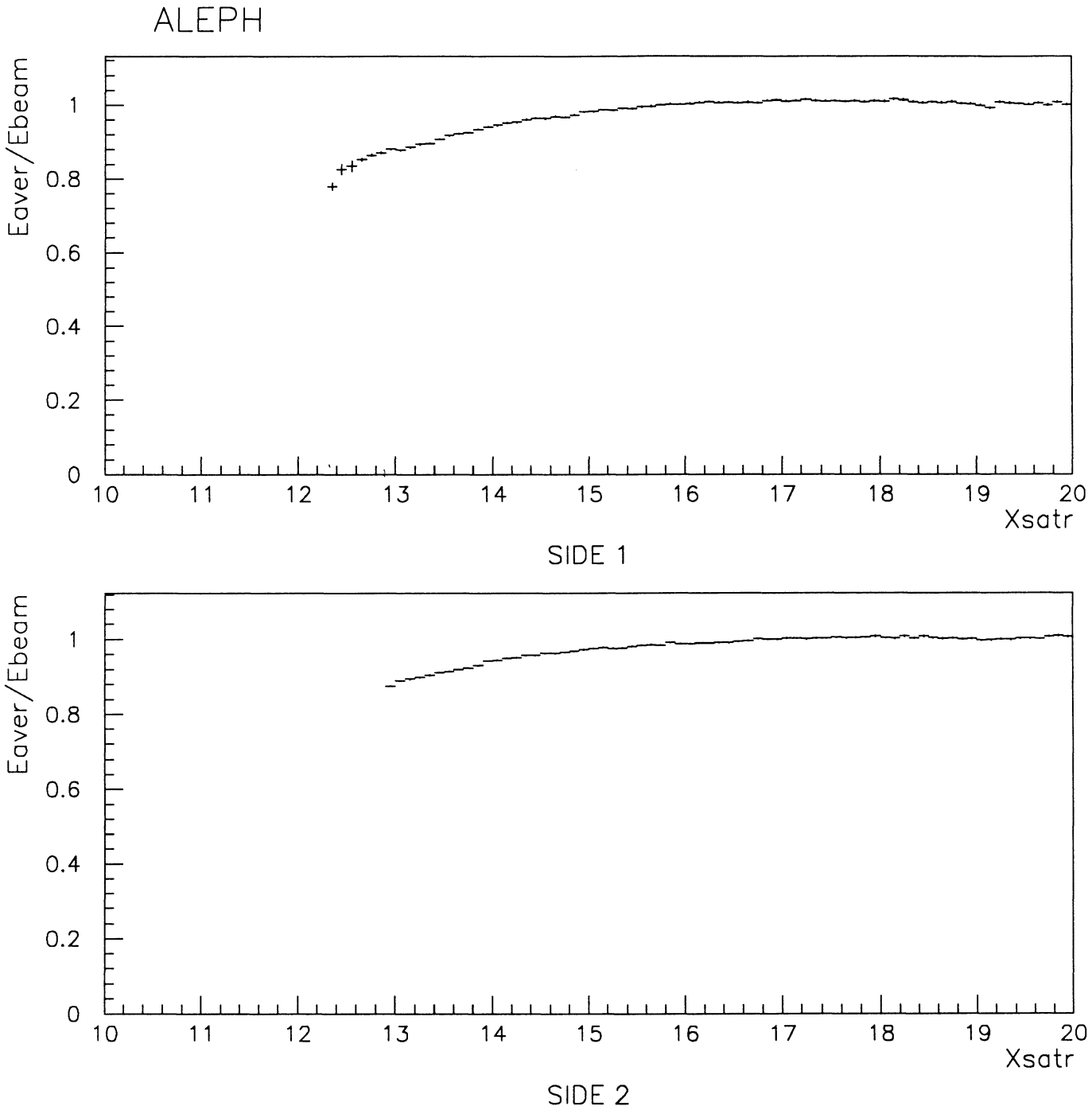
ALEPH
Eaver/Ebeam
0
0.2
0.4
0.6
0.8
1
10
11
12
13
14
15
16
17
18
19
20
Xsatr
SIDE 1
Eaver/Ebeam
0
0.2
0.4
0.6
0.8
1
10
11
12
13
14
15
16
17
18
19
20
Xsatr
SIDE 2

FIGURE 7

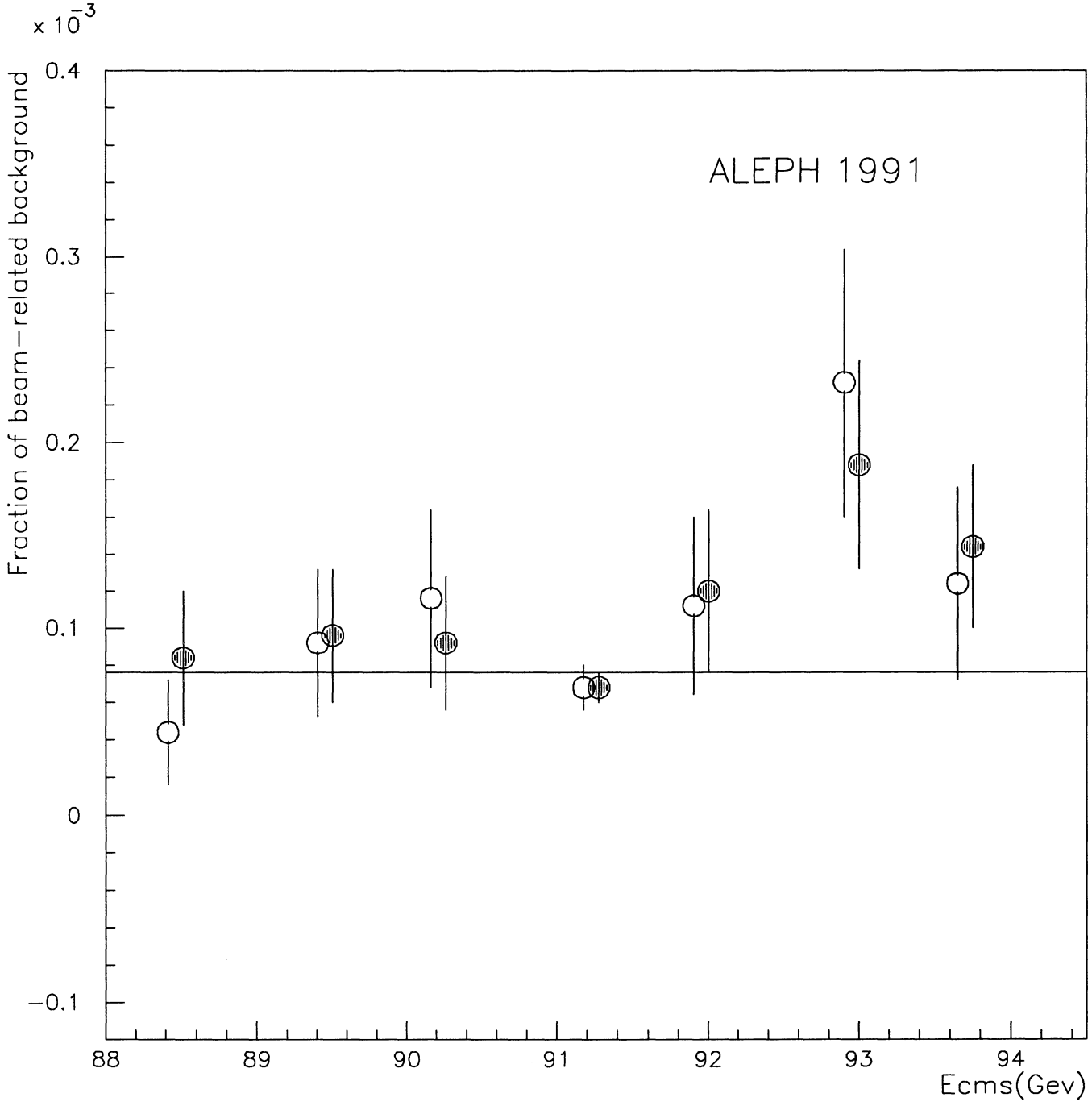
x 10^-3
0.4
0.3
0.2
0.1
0
−0.1
Fraction of beam−related background
ALEPH 1991
88
89
90
91
92
93
94
Ecms(Gev)

FIGURE 8

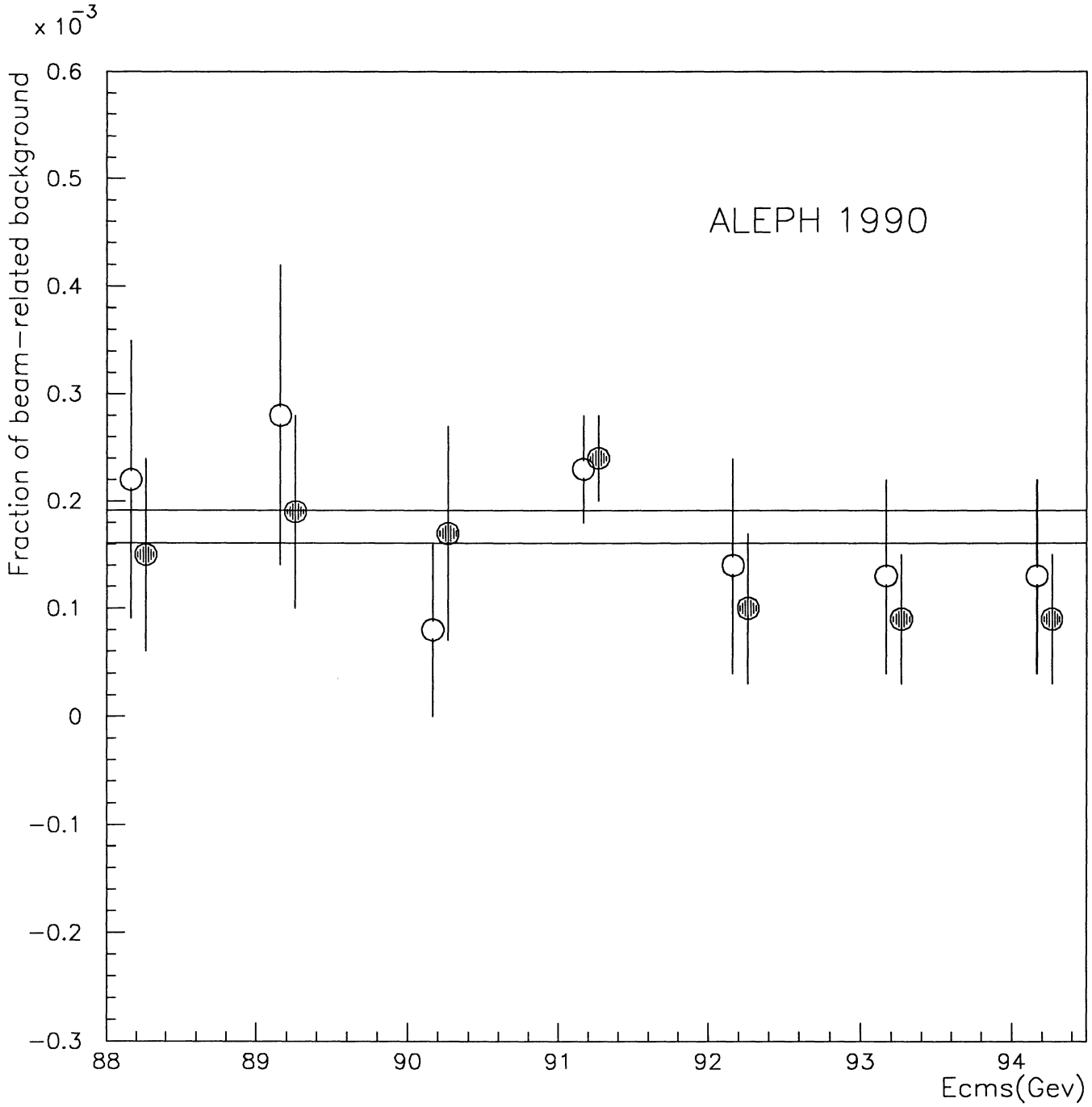
x 10⁻³
0.6
0.5
0.4
0.3
0.2
0.1
0
−0.1
−0.2
−0.3
Fraction of beam−related background
ALEPH 1990
88
89
90
91
92
93
94
Ecms(Gev)

FIGURE 9

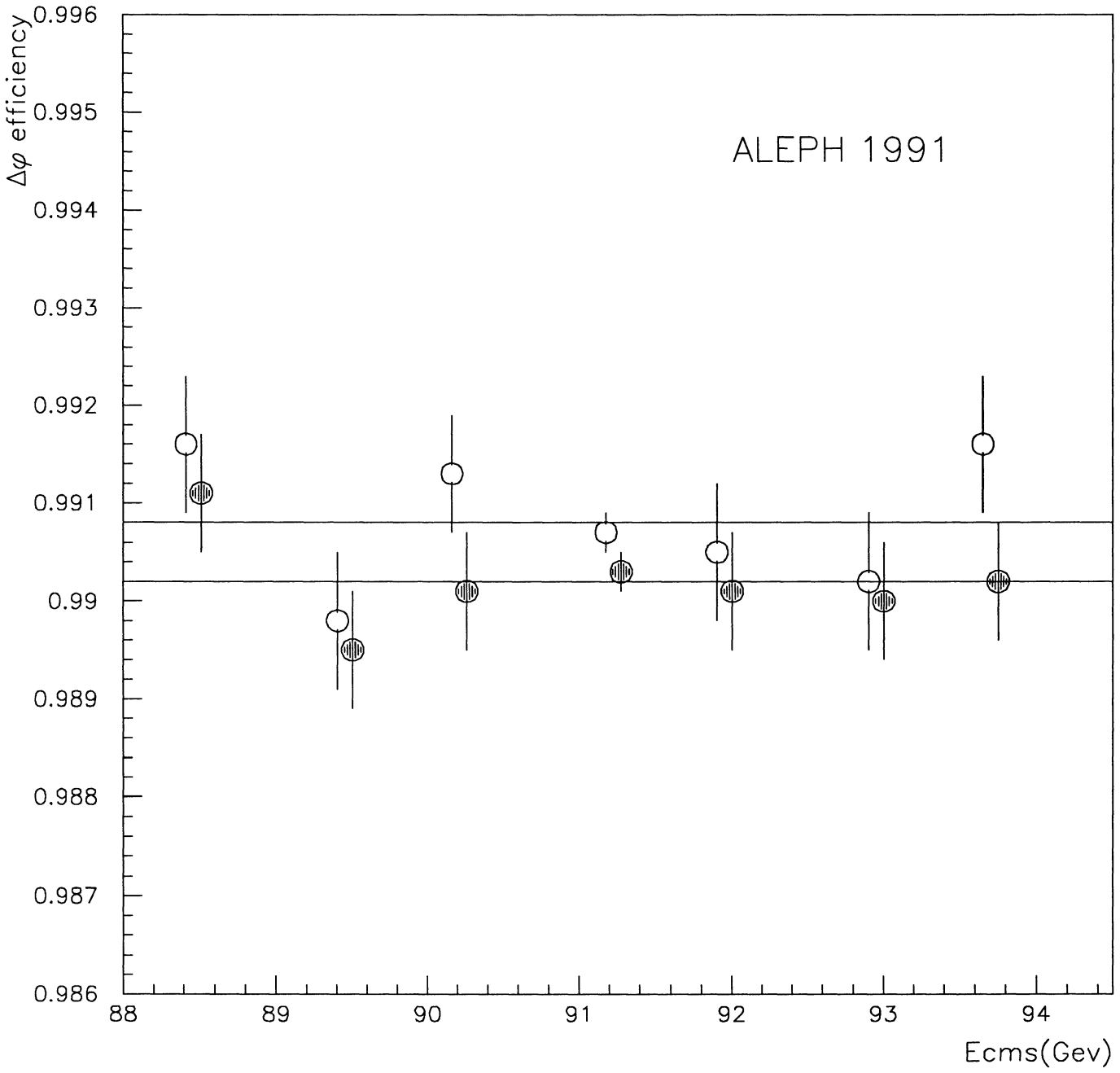
Δφ efficiency
0.996
0.995
0.994
0.993
0.992
0.991
0.99
0.989
0.988
0.987
0.986
ALEPH 1991
88
89
90
91
92
93
94
Ecms(Gev)

FIGURE 10

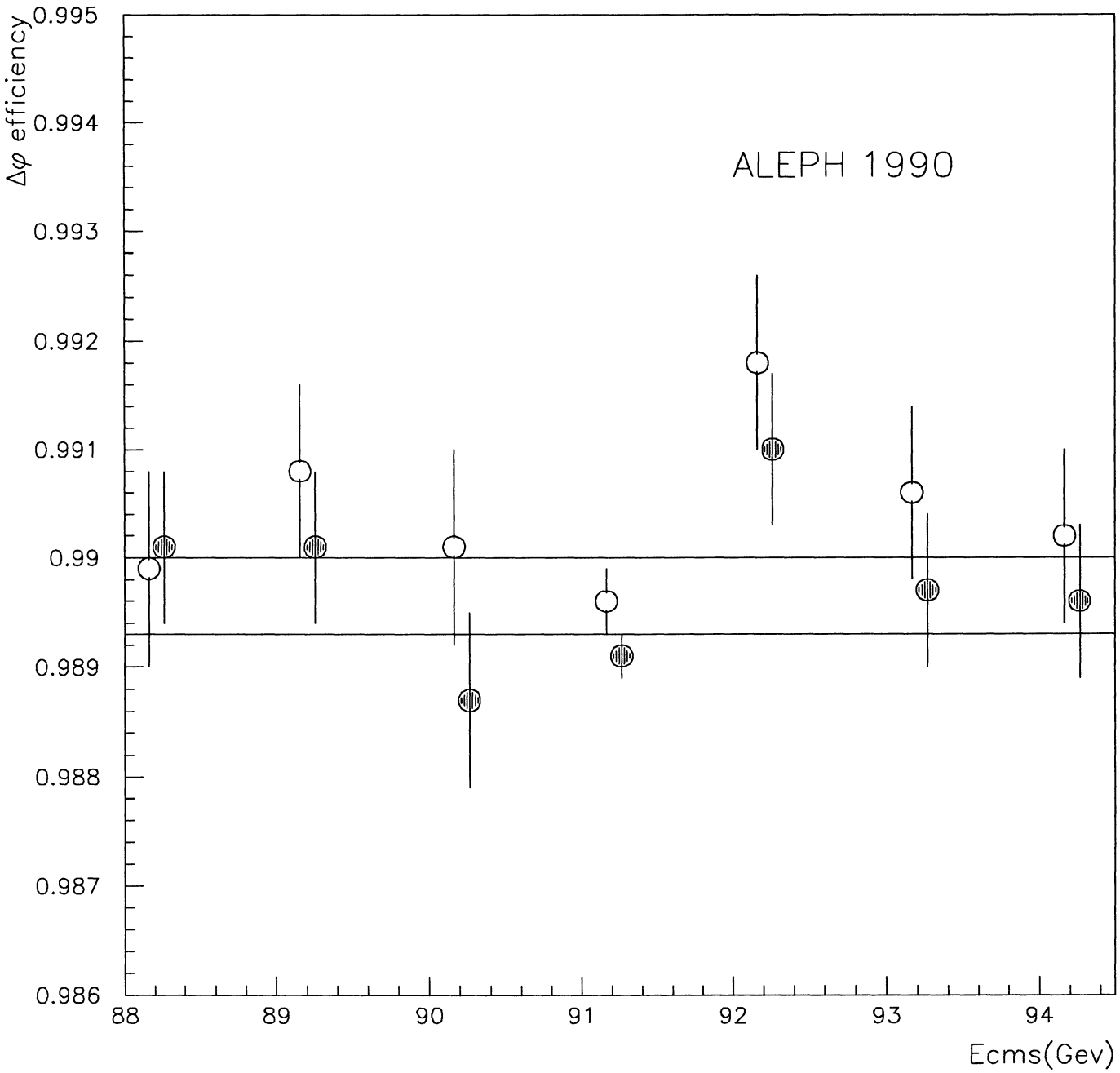
Δφ efficiency
0.995
0.994
0.993
0.992
0.991
0.99
0.989
0.988
0.987
0.986
ALEPH 1990
88
89
90
91
92
93
94
Ecms(Gev)

FIGURE 11

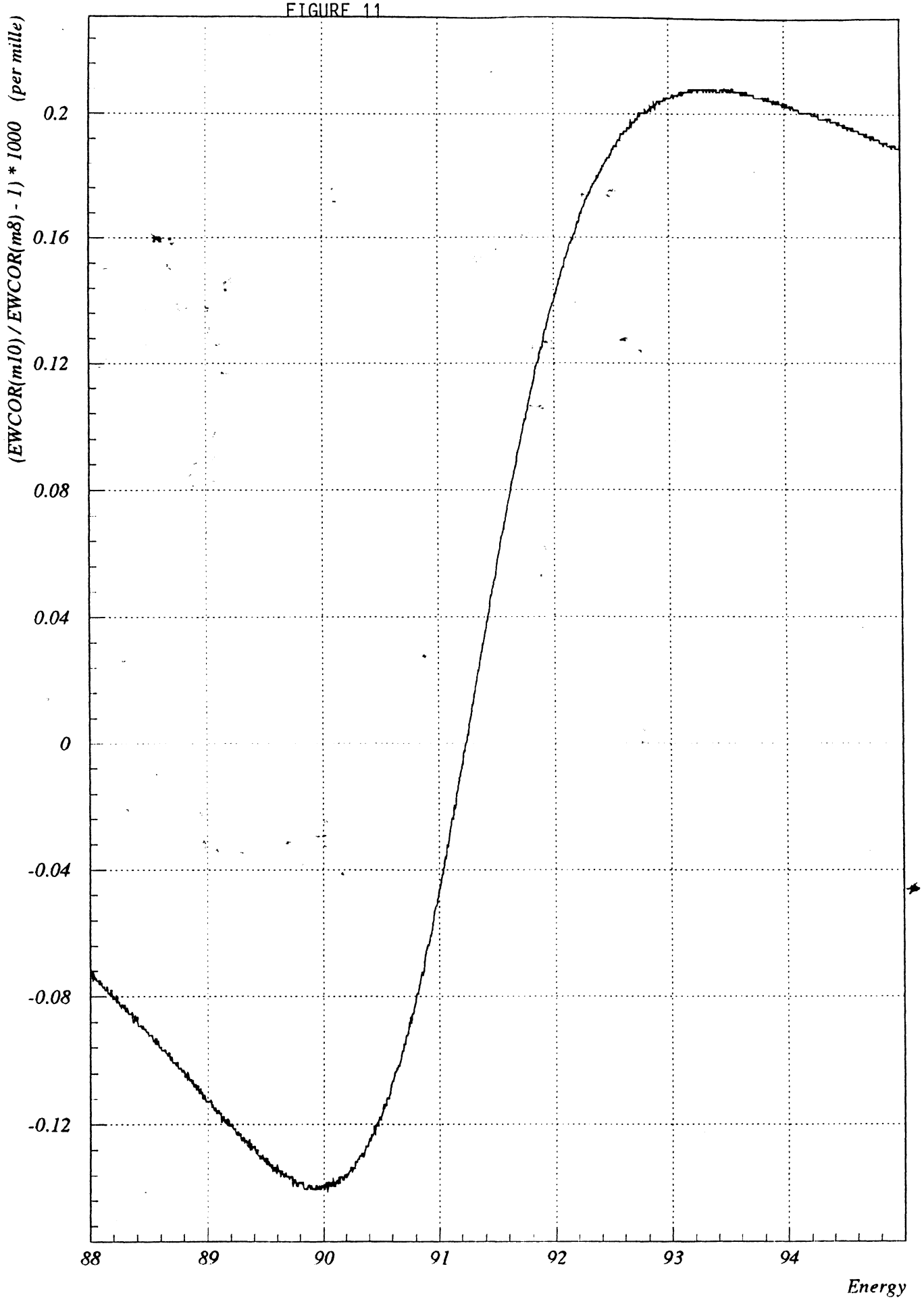
(EWCOR(m10) / EWCOR(m8) - 1) * 1000 (per mille)
0.2
0.16
0.12
0.08
0.04
0
-0.04
-0.08
-0.12
88
89
90
91
92
93
94
Energy

FIGURE 12

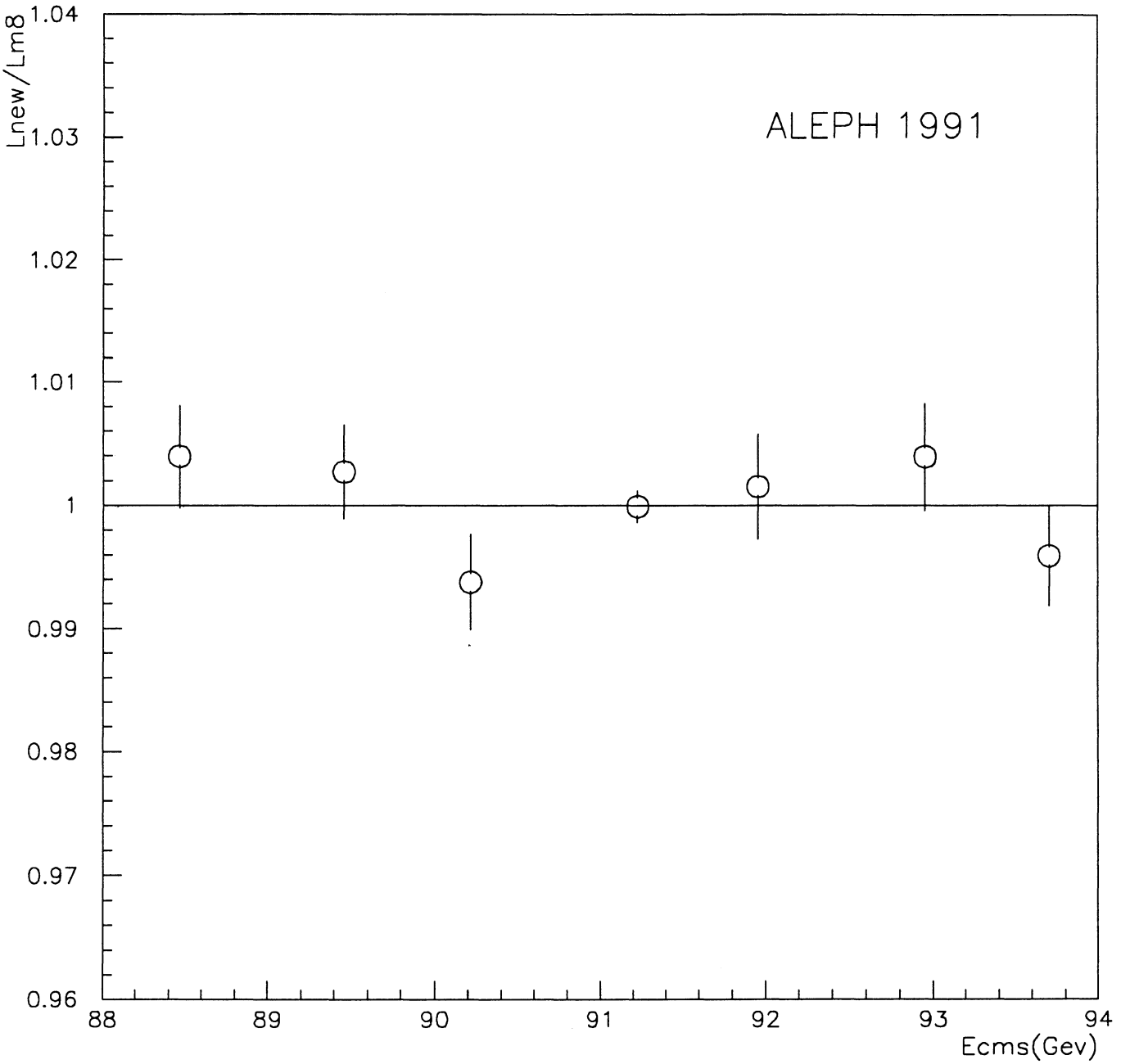
Lnew/Lm8
1.04
1.03
1.02
1.01
1
0.99
0.98
0.97
0.96
ALEPH 1991
88
89
90
91
92
93
94
Ecms(Gev)

FIGURE 13

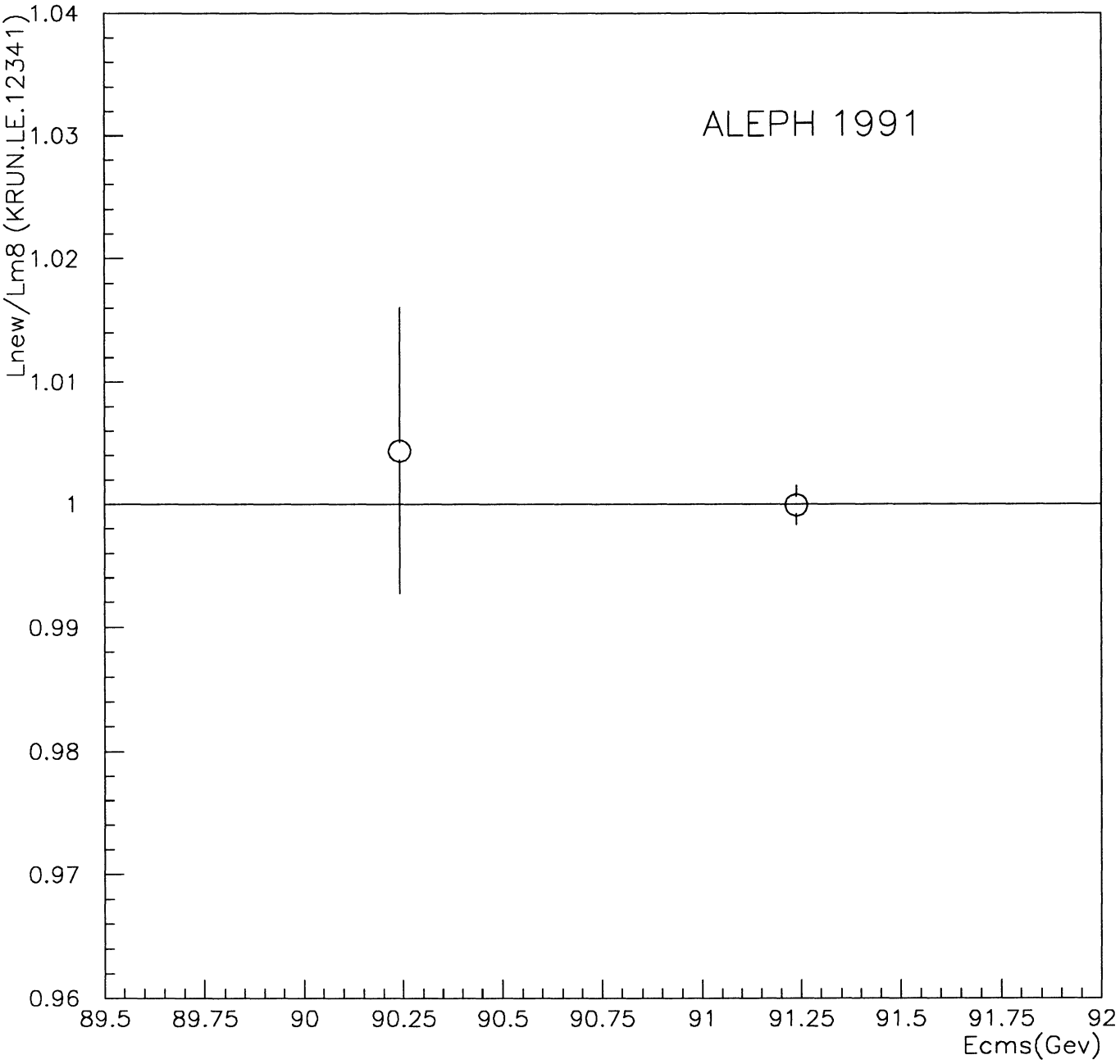
ALEPH 1991
Lnew/Lm8 (KRUN.LE.12341)
1.04
1.03
1.02
1.01
1
0.99
0.98
0.97
0.96
89.5
89.75
90
90.25
90.5
90.75
91
91.25
91.5
91.75
92
Ecms(Gev)

FIGURE 14

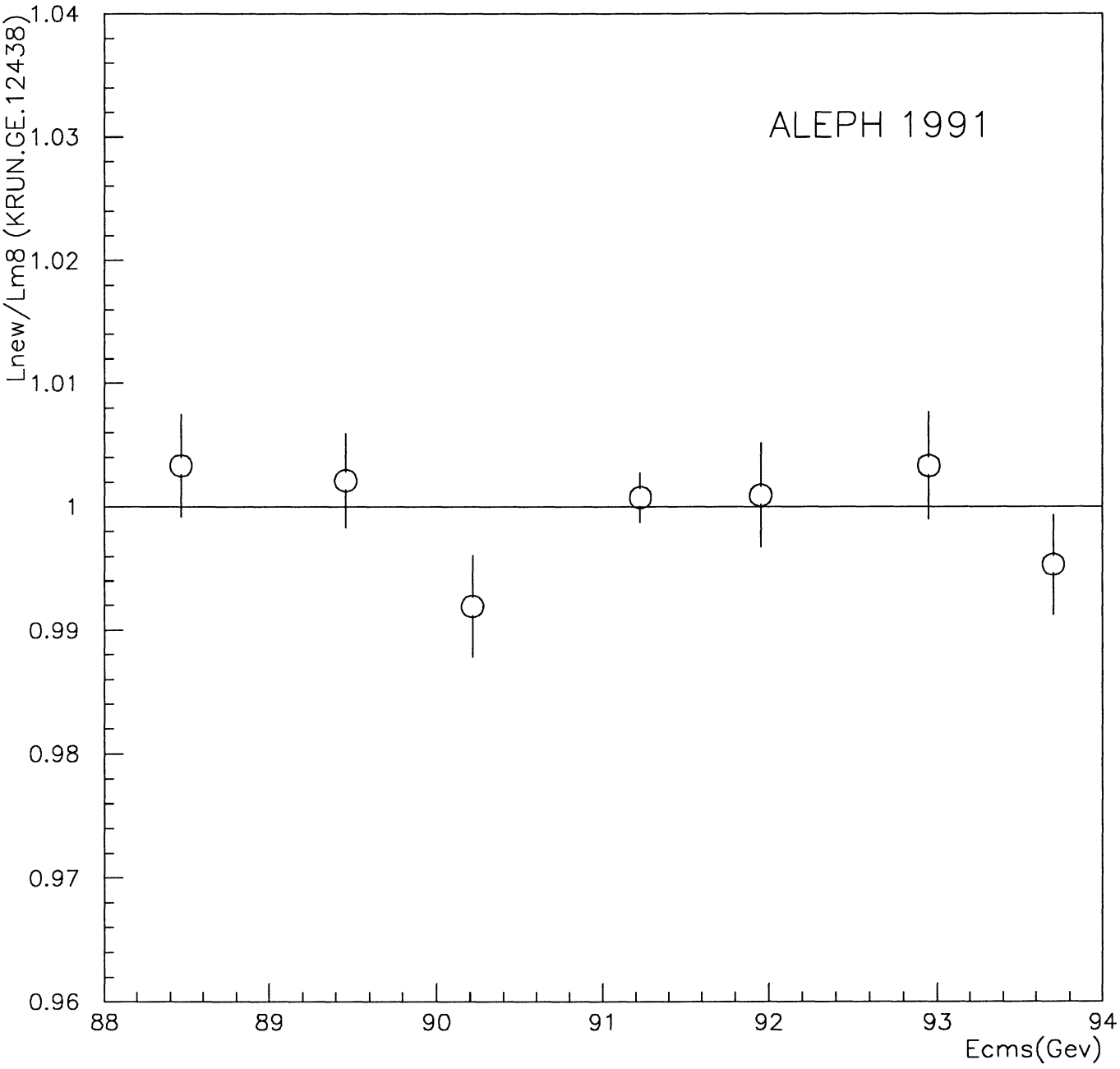
ALEPH 1991
Lnew/Lm8 (KRUN.GE.12438)
1.04
1.03
1.02
1.01
1
0.99
0.98
0.97
0.96
88
89
90
91
92
93
94
Ecms(Gev)

FIGURE 15

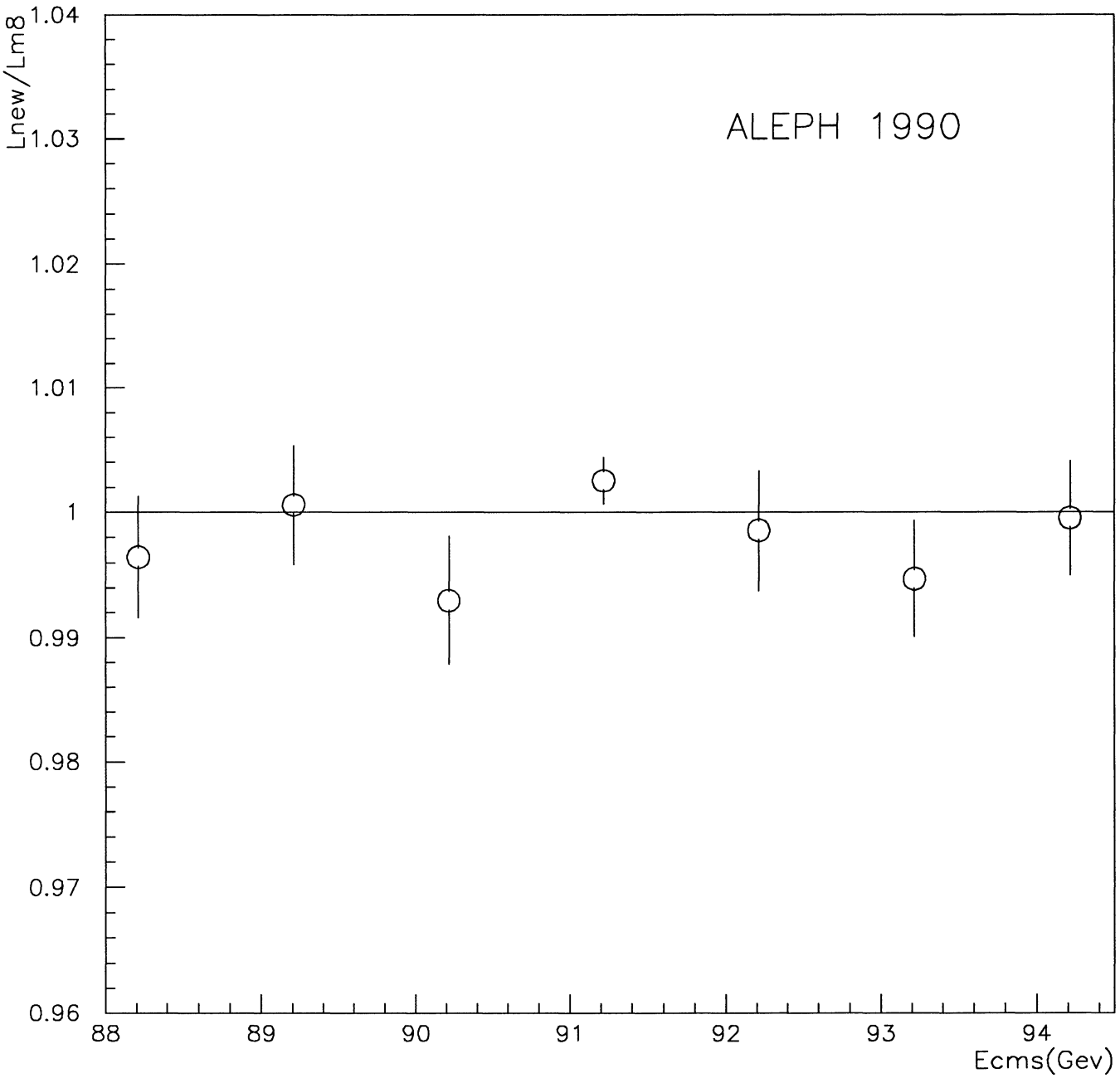
Lnew/Lm8
1.04
1.03
1.02
1.01
1
0.99
0.98
0.97
0.96
ALEPH 1990
88
89
90
91
92
93
94
Ecms(Gev)